Growth of CdSe Nanocrystals by a Catalytic Redox Activation of Ostwald Ripening: A Case Study of the Concept of Traveling Solubility Perturbation

Mauro Epifani,*,† Jordi Arbiol,‡,§ Eva Pellicer,‡ and Joan R. Morante‡

Consiglio Nazionale delle Ricerche - Istituto per la Microelettronica ed i Microsistemi (C.N.R.-I.M.M.), via Monteroni, I-73100 Lecce, Italy, EME/CeRMAE/IN²UB, Departament d'Electrònica, Universitat de Barcelona, C. Martí i Franquès 1, 08028 Barcelona, CAT, Spain, and TEM-MAT, Serveis Cientificotècnics, Universitat de Barcelona, C. Lluìs Solè i Sabaris 1, 08028 Barcelona, CAT, Spain

Received June 11, 2007. Revised Manuscript Received July 24, 2007

Amorphous CdSe nanoparticles were prepared by a room-temperature reaction between selenourea and cadmium nitrate and subsequently crystallized by heating at 145 °C in pyridine. Prolonged heating at this temperature did not result in nanocrystal growth, while the addition, before the heating step, of very small amounts of SeO_2 dissolved in tetrahydrofuran triggered the dissolution of the small initial nanocrystals and the formation of larger particles. The process is controlled by the relative concentrations of SeO_2 and of the capping agent (decanethiol) used in the synthesis of the starting particles. The occurring of an Ostwald ripening mechanism during the treatment with SeO_2 was demonstrated by the evolution of the optical absorption spectra, where the sharp excitonic peaks of the initial small nanocrystals progressively disappeared giving rise to broad peaks at longer wavelengths. The results are interpreted as a fast etching of the nanocrystal surfaces by the formation of Se redox couples, enhancing the dissolution rate of the small nanocrystals and providing new monomers for the growth of larger, crystalline particles. The whole process is interpreted as an example of Ostwald ripening triggered by a moving solubility perturbation.

Introduction

Ostwald ripening is a growth mechanism induced by the differential solubility of particles with a different size, as established by the Gibbs−Thomson principle[1]

$$S_0 = S_\infty \exp(4\gamma_{SL}V_m/RTd)$$

where S_0 is the solubility of the particle with size d, S_∞ is the equilibrium solubility of the substance, γ_{SL} is the interfacial tension of the solid in contact with the solution, V_m is the molar volume, R is the gas constant, and T is the absolute temperature. The Gibbs−Thomson effect prescribes that, at a given temperature, in a system containing a size distribution of particles the smaller particles will have a higher solubility than the larger ones, so they will tend to be completely dissolved with respect to the latter. The dissolution product will redeposit onto the larger particles, resulting in their growth and in a broadening of the size distribution, under low-supersaturation conditions.[1] In an ensemble of particles with a very narrow size distribution the solubility differences will be minimized, and, in the extreme case of a monosized distribution, no Ostwald ripening will occur, an equilibrium being established between the species released and recaptured by the particles. Now, if we suppose that the solubility of some particles in the monosized ensemble is perturbed by an external source, they will be characterized by a new solubility $S' = S_0 + \delta S$, where S_0 is the starting solubility and the δS is the perturbation. An alternative description consists in considering these particles as having an effective size d^* smaller than their actual geometrical size d. The higher solubility of these particles will induce an overall differential solubility in the system, so triggering Ostwald ripening. In particular, the species coming from their dissolution will be deposited onto some unperturbed particles, changing their size and, hence, their solubility. If the perturbation is extinguished after affecting a single particle, then, depending on the perturbation concentration, it may happen that the overall concentration of newly formed species will slightly affect the size distribution of the ensemble and the growth phenomena will be hindered. On the other hand, if the perturbation is not consumed in the particle dissolution, it becomes a traveling perturbation, propagating through the ensemble, enhancing the dissolution rates of an increasing number of particles and the overall growth rate.

These general considerations do not have a purely theoretical origin but were suggested by the observations of the phenomena occurring during the heating of CdSe suspensions prepared in a previous work[2] from the room-temperature reaction between selenourea and cadmium

* Corresponding author e-mail: mauro.epifani@le.imm.cnr.it.
† Istituto per la Microelettronica ed i Microsistemi (C.N.R.-I.M.M.).
‡ Departament d'Electrònica, Universitat de Barcelona.
§ Serveis Cientificotècnics, Universitat de Barcelona.

(1) (a) Sugimoto, T. *Adv. Colloid Interface Sci.* **1987**, *28*, 65−108. (b) Mullin, J. W. *Crystallization*; Elsevier Butterworth-Heinemann: Oxford, U.K., 2001.

(2) Epifani, M.; Giannini, C.; Manna, L. *Mater. Lett.* **2004**, *58*, 2429−2432.

10.1021/cm071556p CCC: $37.00
Published on Web 09/11/2007

nitrate. In the investigation of the reproducibility of the process, we had discovered that remarkable changes in the growth of the nanocrystals could occur in the same synthesis conditions. A series of control experiments led us to the conclusion that this effect was due to hardly detectable oxidation of selenourea, and we tested this hypothesis by introducing controlled amounts of SeO_2 in the starting suspension of CdSe nanocrystals prepared by extremely pure selenourea. In this work we show the results of this study, where we provide evidence for a redox activated Ostwald ripening mechanism for the growth of nanocrystals, corresponding to the general description provided above.

Experimental Section

(a) Preparation and Crystallization of Starting Nanoparticles. A suspension of amorphous CdSe nanoparticles was prepared as follows. In a glovebox thoroughly purified from oxygen, 25 mg of selenourea (98%, Aldrich) and 65 mg of $Cd(NO_3)_2 \cdot 4H_2O$ (98%, Aldrich) were separately dissolved in 1 mL of dimethyl sulfoxide (DMSO, 99.7%, Acros Organics) and then mixed. After 1 min, 25 μL of a concentrated (30 wt % in water) ammonia solution were rapidly injected, and the solution suddenly became yellow. After 2 min since the base addition, various volumes (typically 5 μL) of decanethiol (96%, Aldrich) dissolved in 2 mL of tetrahydrofuran (THF, 99.9%, Aldrich) were added, and the opaque slurry was further stirred for 2 min. Finally, the slurry was transferred to a centrifugation cuvette, where heptane was added, resulting in the immediate expulsion of the nanoparticles from the slurry, followed by centrifugation. The yellow precipitate was dispersed in 12 mL of pyridine (99%, Aldrich), forming a clear, deep yellow solution. The vial was then immersed in a bath at 145 °C and kept there for 30 min, after which it was extracted from the bath and cooled to room temperature. A clear, yellow solution was obtained.

(b) Growth Experiments. Before the above-described heating step in the bath, various amounts of a solution of 50 mg of SeO_2 (99.9%, Aldrich) in 5 mL of THF were added. Then the vial was closed and immersed in the bath at 145 °C. The solution color changed from yellow to orange or deep red, with the color change rate and the final color depending on the decanethiol concentration used in the synthesis of the starting nanoparticles and on the SeO_2 concentration. After various times, the vial was extracted from the bath and cooled. All the growth experiments were carried out in light.

(c) Nanocrystal Extraction and Characterization. After the heating step, the nanocrystals were extracted from the pyridine suspension according to various procedures. For optical and X-ray diffraction (XRD) characterizations, the extraction was carried out by addition of dodecanethiol to the nanocrystals suspensions, resulting in the flocculation of the functionalized nanocrystals. They were then dissolved in toluene for optical absorption measurements (Varian, Cary 5E) or dried for XRD measurements, carried out with a Siemens D-500 diffractometer, using the Cu Kα radiation (λ = 1.5418 Å). In the case of the smallest nanocrystals, prepared without the addition of SeO_2 during the heating step (see section (a) above), the extraction was carried out by addition of heptane, resulting in the slow flocculation of nanocrystals, and then collected by centrifugation. This different procedure was necessary for transmission electron microscopy (TEM) observations on such nanocrystals, since those functionalized with dodecanethiol became amorphous under the TEM beam.

The structural and morphological characterization of the various nanocrystals was carried out by means of transmission electron microscopy (TEM) and selected area electron diffraction (SAED). In order to obtain the high-resolution TEM (HRTEM) results we used a field emission gun microscope Jeol 2010F, which works at 200 kV and has a point-to-point resolution of 0.19 nm. The software used for digital image analysis and crystallographic indexation was the Digital Micrograph (Gatan) and Carine, respectively. The samples for the TEM observations were prepared by placing a drop of nanocrystals suspensions in hexane onto a carbon coated copper grid, followed by drying.

Results and Discussion

In an early series of growth experiments,[2] nanocrystals with different sizes were prepared by simply changing the decanethiol concentration in the synthesis of the starting particles and then heating the resulting suspension without any SeO_2 added. Suspensions with colors ranging from yellow to orange to red were obtained, according to the final nanocrystal size. In the following series of experiments carried out exactly in the same conditions, instead, the yellow color of the initial suspension did not change even after prolonged heating at 145 °C. After a series of control experiments, it was discovered that the only difference in the two series of experiments was the use of very fresh selenourea in the second series. This observation suggested that any color change of the suspensions during the early heating experiments was entirely due to impurities from selenourea degradation. For confirming the selenourea role, a series of growth experiments was carried out where a controlled amount of SeO_2 was added to the initial suspension before the heating stage, as described in the Experimental Section. Simultaneously, each time a suspension with no addition of SeO_2 was heated, this acted as an internal standard test for ensuring that the selenourea was not degraded. The choice of SeO_2 was dictated by the consideration that selenourea is very easily oxidized and that the supposed impurities could be due to its surface oxidation. Thus SeO_2 seemed suitable to simulate the effect of surface oxidation of selenourea.

The results of the growth experiments confirmed the role of SeO_2, since depending on its concentration and on the heating time differently colored suspensions were obtained. In Figure 1 the optical absorption spectra are reported for selected suspensions, whose synthesis parameters are reported in Table 1. The right panel of the figure will be referred to in the discussion about the growth process (see below), and here we will refer only to the left panel. Curve A refers to the starting nanoparticles described in section (a) of the Experimental Section and was unchanged even for different heating times.

A very similar curve has already been reported for CdSe nanocrystals having a size of about 17 Å.[3] The sharp excitonic peaks in the inset appear after the heating step, while before heating the curve showed only an increasing featureless absorption at short wavelengths. Since before heating the particles are amorphous, the appearance of the peaks below 420 nm was considered as an indication of

(3) (a) Murray, C. B.; Kagan, C. R.; Bawendi, M. G. *Annu. Rev. Mater. Sci.* **2000**, *30*, 545−610. (b) Artemyev, M. V.; Woggon, U.; Jaschinski, H.; Gurinovich, L. I.; Gaponenko, J. *J. Phys. Chem. B* **2000**, *104*, 11617−11621.

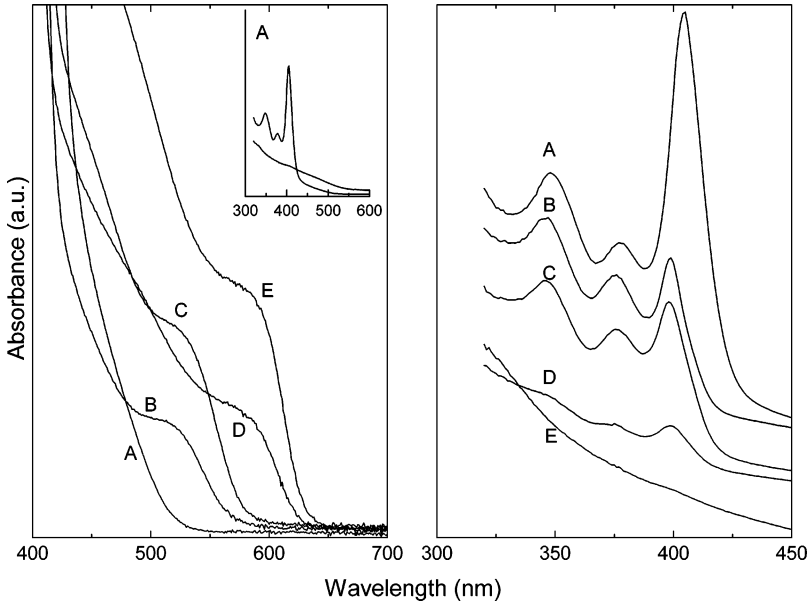

Figure 1. Optical absorption spectra measured on CdSe suspensions heated at 145 °C and prepared as described in Table 1. The inset in the left panel shows the short-wavelength part of curve A before (bottom curve) and after (top curve) the heating step. The right panel reports the high-energy flank of the curves, vertically displaced for clarity.

Table 1. Synthesis Parameters for the Samples in Figure 1

curve	decanethiol in initial synthesis (μL)	SeO_2 solution (μL)	heating time (min)
A	5	0	30
B	15	50	30
C	15	200	30
D	5	200	30
E	5	600	10

particle crystallization. Decanethiol is very effective in limiting the growth of the starting particles, before the crystallization step. This conclusion is suggested by the comparison of the optical absorption curves of samples prepared: with decanethiol addition during the synthesis, as described in section (a) of the Experimental Section, or with decanethiol addition not in the synthesis but just before the heating step (see Figure S1, Supporting Information). Since the decanethiol/Cd molar ratio is only about 10^{-1}, this result suggests strong bonding of the thiol molecules to the Cd surface atoms. Comparison of the two curves in Figure S1 indicates also that a bimodal size distribution could be present, with very small clusters that, in the case of delayed addition of decanethiol, may further aggregate to the larger species, with the consequent quenching of the corresponding absorption peak (at about 377 nm, see Figure S1). On the other hand, it is remarkable that a peak at about 348 nm is less affected than the peak at 377 nm, in agreement with the attribution of such peak to magic number clusters,[4] for which a remarkable stability is expected.

Summarizing, the use of decanethiol in the preparation of the initial suspension provides, after the heating step (curve A in Figure 1), CdSe nanocrystals with a size of 17 Å, with the possible coexistence of very small clusters. When the SeO_2 solution was added, larger nanocrystals were formed, as evidenced by the red-shift of the absorption peak in Figure 1. The XRD and TEM results shown below indeed confirm that the nanocrystals size increases from about 1.7 to 3.5 nm from curve A to curve E (this mean size for sample E was determined by the TEM studies), while a size of about 2.9 nm was found from the XRD pattern of sample C (Figure S2, Supporting Information). Observing in detail the spectra, it is seen that larger concentrations of decanethiol in the initial synthesis resulted in smaller nanocrystals, even using the same SeO_2 concentration and heating times (comparing curves C and D), while increasing SeO_2 concentrations resulted in growth of larger nanocrystals (comparing curves A, D, and E), from 1.7 to 3.5 nm. These results ultimately show the influence of even small concentrations of SeO_2 in triggering the particle growth. Indeed, we have observed that growth takes place even at 70 °C within 3 h and even at room temperature but on a time scale of a few months.

The formation of crystalline products after the heating stage was clearly confirmed by XRD measurements on dried nanoparticles prepared with 5 μL of decanethiol, a heating time of 10 min, and differing only for the SeO_2 concentration in the heating step. This series of experiments was differently designed from the syntheses in Figure 1, and it was aimed to specifically evidence the role of SeO_2 concentration in changing the initial particle size, so all the other synthesis parameters were kept fixed.

The related XRD patterns are shown in Figure 2. We note that samples A and D are the same of samples A and E in Figure 1, respectively (actually sample A in Figure 1 was heated for 30 min, but its optical absorption curve and XRD pattern is identical to that of sample A in Figure 2, as expected from the remarkable stability of these nanocrystals). The patterns show the presence of CdSe nanocrystals in the usual hexagonal (wurtzite) crystallographic phase.[5] The particle size increases with increasing the SeO_2 concentration,

(4) (a) Soloviev, V. N.; Eichhofer, A.; Fenske, D.; Banin, U. *J. Am. Chem. Soc.* **2001**, *123*, 2354−2364. (b) Peng, Z. A.; Peng, X. *J. Am. Chem. Soc.* **2002**, *124*, 3343−3353.

(5) JCPD card 02-0330, 1997. Space group: *P63mc* (wurtzite), $a = b =$ 0.430 nm, $c = 0.702$ nm, and $\alpha = \beta = 90°$, $\gamma = 120°$.

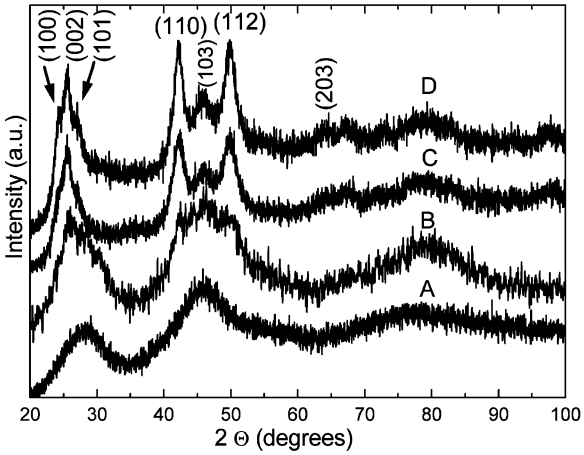

Figure 2. XRD patterns measured on suspensions prepared with 5 μL of decanethiol in the initial synthesis, heated at 145 °C for 10 min, and with (A) no SeO_2 added and (B) 100 μL, (C) 300 μL, and (D) 600 μL of SeO_2 solution in THF, respectively.

Table 2. Mean Nanocrystal Size in Samples of Figure 2

sample	size (nm)
A[a]	1.7
B[a]	2.2
C[b]	3.1
D[b]	3.9

[a] From comparison with ref 3. [b] From the Scherrer analysis of the (110) reflection.

as indicated by the peak narrowing and the increased peak resolution. This result is confirmed by the size obtained from the analysis of the XRD patterns, summarized in Table 2. HRTEM studies on representative samples were carried out for further structural elucidation of the nanocrystals. The samples corresponding to patterns A and D in Figure 2 were chosen, as representative of the two size extremes. Functionalized nanocrystals of sample A became amorphous under the TEM beam, and we could only record the SAED pattern, showing their crystalline nature (Figure S3, Supporting Information). We tried to carry out observations on the dried nanocrystals, as extracted from the pyridine solution after the growth experiment. The extraction by heptane takes place by removal of the pyridine capping so aggregation occurred.

The TEM studies on such samples confirmed the presence of CdSe nanocrystals in the hexagonal phase, with sample A containing very small particles, as shown by the diffuse rings in the corresponding SAED pattern (Figure 3).

A careful size determination was not easy, due to nanocrystals aggregation, but when the lattice fringes corresponding to different nanocrystals can be more clearly distinguished (Figure S4, Supporting Information) the corresponding domains have a size of about 4 nm, much larger than expected from the XRD pattern and from the optical absorption curve (this phenomenon was also observed in the observation of not functionalized nanocrystals of sample D and could be related just to the lack of a surface capping layer).

In the case of sample D, the extracted nanocrystals were functionalized with trioctylphoshine instead of dodecanethiol, resulting in stability under the TEM beam, and dispersed in hexane. The results of TEM analysis are shown in Figure 4.

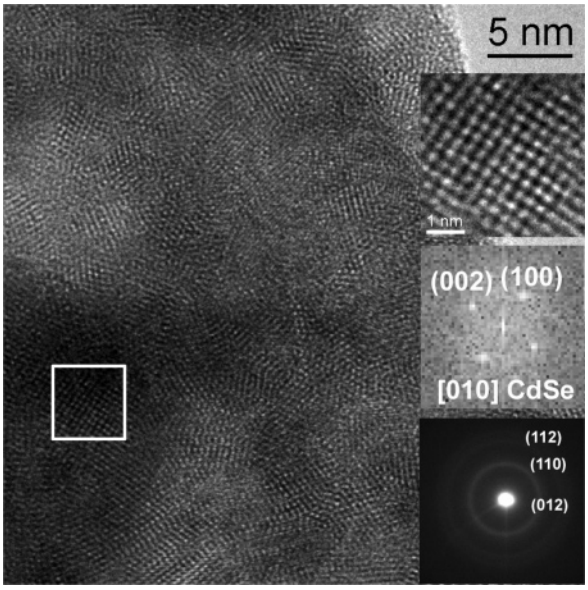

Figure 3. HRTEM image of sample A in Figure 2 and, from top to bottom, higher magnification of the nanocrystal marked in white, related power spectrum and a SAED pattern of the sample.

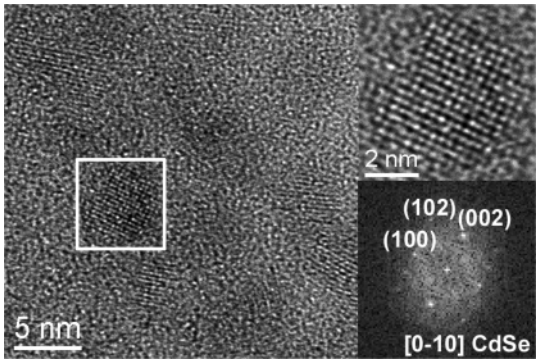

Figure 4. HRTEM image of functionalized nanocrystals of sample D in Figure 2 and, at the right, magnified detail of the squared single nanocrystal and related power spectrum.

Nanocrystals with a mean size of 3.5 ± 1 nm are clearly distinguished, in good agreement with the XRD results in Table 2. Some nanocrystals display a remarkable lattice distortion (Figure S5 reports an example, observed in the same sample D), but again the crystallographic phase is the hexagonal.

After ensuring the formation of CdSe nanocrystals and clearly establishing the influence of the SeO_2 concentration, the next step was to obtain an overview of the nanocrystal formation process. From this point of view, the growth experiments described in Table 1 were essential, since they span a set of synthesis conditions where the effect of SeO_2 is progressively enhanced: at first no SeO_2, then insertion of SeO_2 with higher decanethiol concentrations, and finally increasing SeO_2 with decreased decanethiol.

When observing the right panel curves in Figure 1, the peaks characteristic of the nanocrystals prepared without SeO_2 (curve A) become progressively less intense from curve B to D and completely disappear in curve E. Since, from the previous XRD and TEM results, the nanocrystal size in sample A is 1.7 nm, 2.9 nm in sample C, and 3.5 nm in sample E, we have a clear picture of an Ostwald ripening mechanism, with the largest particles that grow at the expense

of the total consumption of the smallest ones. In the absence of SeO_2 the starting suspensions are simply collections of particles with a narrow size distribution, and, accordingly with the general concepts exposed in the Introduction, prolonged heating of the starting suspensions did not result in any growth. Instead, when the SeO_2 solution was added, growth occurred, and the starting particles began to be etched, as shown by the blue-shift of the high-energy peaks in Figure 1 from curve A to curve B to curve D. It is now concluded that the Ostwald ripening mechanism is triggered by the presence of SeO_2. In particular, some particles are dissolved at a rate depending on the decanethiol and on the SeO_2 concentrations, creating monomers for the growth of larger particles. The growth of larger particles may occur by release of the supersaturation of monomeric species created by the dissolution of the small particles. However, this process seems kinetically unlikely at the heating temperature of 145 °C, thus we assume that particle growth occurs by reprecipitation of the dissolution products onto other nanocrystals, acting as seeds and favoring the formation of crystalline products. The occurrence of Ostwald ripening also explains the broadening of the particle size distribution in the growth experiments, as revealed from the TEM data on sample D, where a size distribution is clearly revealed, in contrast with the monodispersed feature of sample A. It remains to be studied the reason for nanocrystals etching due to the SeO_2 addition. In their recent work on the ething of CdSe nanocrystals, Li et al.[6] have proposed the oxidation of surface Se^{2-} to SeO_2 by oxygen dissolved in the suspension, followed by reduction to Se^0 by 3-amino-1-propanol, where the nanocrystals are dispersed, and by disproportionation to Se^{2-}, which provides the source for further particle growth. Nevertheless, despite the fact that we directly introduce SeO_2 in our growth suspensions, we have to invoke a different mechanism in our system: a sample was prepared like sample D in Figure 1 but using toluene instead of pyridine. Since pyridine should have the same role of 3-amino-1-propanol, in its absence a more hindered growth would be expected. Actually, after less than 1 min since the immersion in the bath, the initially yellow-orange precipitate (the initial nanoparticles are not soluble in noncoordinating toluene) became deep red, and the extracted product was crystalline (Figure S6). It results that pyridine is unnecessary for triggering the etching mechanism, but, on the other hand, it is fundamental as a growth regulator by bonding to the particle surface. As a further control experiment, $SeCl_4$ was used instead of SeO_2 in a growth experiment, but in this case a brown-yellow precipitate formed. Thus even the oxygen of the Se oxide seems to have a role in the etching process.

Putting together all these observations, we propose an etching scheme summarized in Figure 5. First the selenium atom in SeO_2 attacks the Se^{2-} on the particle surfaces, beginning an electron transfer from the latter to the SeO_2 selenium, aided by the large difference in the two Se

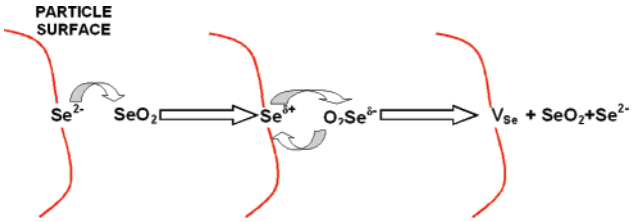

Figure 5. Suggested pathway of the etching process of the nanocrystal surface.

oxidation states. The consequent increasing negative charge on the SeO_2 selenium further pushes back the electron density in SeO_2 toward oxygen. The latter then acquires a higher negative charge density, and this process may facilitate the oxygen bonding to the surface Se^{2-} which has acquired a partial positive charge with respect to the situation before the etching process. This process, in turn, allows the electron flow from the surface Se to the SeO_2 selenium to continue. At the end, the selenium atom from the surface bonds with the oxygen from SeO_2, while Se from SeO_2 is introduced in the solution like Se^{2-}. SeO_2 is then regenerated and can begin a new attack, so low concentrations of SeO_2 are sufficient for extensive etching. In this scheme the two Se species at the end of the process have exchanged their role. The driving force of the process is attributed to the electrochemical free energy difference between the two Se species, which can be further changed by the reaction temperature and other factors. The etching proceeds eventually to the inner Se^{2-} species in CdSe particles, until they are made unstable and completely dissolved. The various species are redeposited onto existing nanocrystals in the suspensions acting as seeds for the formation of larger nanocrystals. The Cd species carrying the decanethiol ligand can stop this process by deactivating the surface sites where they are deposited, which would explain the hindering of growth by larger decanethiol concentrations. The latter is a similar mechanism to that proposed by Li et al.[6c] who attribute to the formation of Cd hydroxides or amine complexes the etching plateau observed during their experiments. We underline that we have proposed just a reaction hypothesis, where the species actually involved are not clearly identified. For instance, SeO_2 has a structure constituted by polymeric chains,[7] and it is unlikely that dissolution in THF may modify it, so depicting a single SeO_2 molecule in the reaction scheme is only indicative.

We have shown that the Ostwald growth occurs by a solubility perturbation by the addition of SeO_2 in the starting suspension. Moreover, the SeO_2 concentration is very low (the atomic ratio of Se in SeO_2 to that in CdSe is about 10^{-2}), and it is necessary to suppose that the species responsible for the dissolution are not consumed in the process (catalytic effect) and that they can move from one particle to another (since from the results in the right panel of Figure 1 it appears that the initial small particles are completely consumed). From the analysis of this process we concluded, on a more general ground, about the possibility of triggering Ostwald ripening by traveling solubility perturbations, as exposed in

(6) (a) Li, R.; Lee, J.; Kang, D.; Luo, Z.; Aindow, M.; Papadimitrakopoulos, F. *Adv. Funct. Mater.* **2006**, *16*, 345−350. (b) Li, R.; Lee, J.; Yang, B.; Horspool, D. N.; Aindow, M.; Papadimitrakopoulos, F. *J. Am. Chem. Soc.* **2005**, *127*, 2524−2532. (c) Li, R.; Luo, Z.; Papadimitrakopoulos, F. *J. Am. Chem. Soc.* **2006**, *128*, 6280−6281.

(7) Greenwood, N. N.; Earnshaw, A. *Chemistry of the Elements*, 2nd ed.; Butterworth-Heinemann: Oxford, 1997; p 779.

the Introduction in the form of a purely theoretical speculation.

We have observed that the growth phenomena do not need a basic solvent, light (samples kept in the dark in environments where visible light was moreover rigorously excluded allowed determining that growth occurred even in the dark), and temperature, that both amorphous and precrystallized starting suspensions can be used for the growth experiments, and that SeO_2 can be dissolved in THF or methanol or directly added to the suspensions. So the etching process is extremely favored in a broad range of conditions and occurs by a direct attack of the nanoparticle surfaces at remarkable rates. The pyridine environment can provide a tool for controlling the growth rate, but in no way can it stop the etching process. The reason for the remarkable difference with the etching processes previously reported is still unclear, even though the very small size of the initial nanocrystals can provide particularly active surfaces.

Conclusions

In this work it has been shown, using CdSe nanocrystals as a case study, that growth by Ostwald ripening can be activated by small migrating solubility perturbations of the starting nanocrystals. In particular, (a) the dissolution of the initial nanocrystals can be catalytically activated by the introduction of very small amounts of a suitable redox couple in the starting solution; (b) the existence of Ostwald ripening phenomena is explicitly shown by the evolution of the sharp excitonic peaks of the starting nanocrystals; and (c) the activation mechanism is different from those previously proposed in other etching studies, and oxygen, water, temperature, light, and a base do not appear as essential in triggering the growth, but, of course, an influence of the reaction kinetics cannot be excluded a priori.

Since the case of CdSe appears as a particular case of a general mechanism, as described in the Introduction, a fast growth of large nanocrystals starting from smaller ones could occur for other systems, if suitable redox couples can be found for each system. Further perspectives include the growth in the presence of ligands that can selectively adsorb onto determined surfaces, resulting in anisotropic growth.

Acknowledgment. The authors thank the XRD unit of the Serveis Científicotècnics of the University of Barcelona for its cooperation.

Supporting Information Available: Optical absorption curves on as prepared suspensions, TEM images of functionalized and nonfunctionalized nanocrystals, and XRD pattern on nanocrystals grown in toluene. This material is available free of charge via the Internet at http://pubs.acs.org.

CM071556P